UPPSALA
UNIVERSITET

FREIA Report 2021/05
CERN-ACC-NOTE-2021-0032

DEPARTMENT OF PHYSICS AND ASTRONOMY
UPPSALA UNIVERSITY

Proof-of-principle of the ultra-narrowband detection scheme at 30 GHz toward weakly interacting slim particle search

A. Miyazaki[1,2], F. Caspers[2,3], J. Steinmann[4], T. Ruess[4], J. Jelonnek[4]

[1]Uppsala University, Uppsala, Sweden
[2]CERN, Switzerland
[3]European Scientific Institute, France
[4] Karlsruhe Institute for Technology, Germany

Department of
Physics and Astronomy
Uppsala University
P.O. Box 516
SE – 751 20 Uppsala
Sweden

Proof-of-principle of the ultra-narrowband detection scheme at 30 GHz toward weakly interacting slim particle search

A. Miyazaki[1,2], F. Caspers[2], J. Steinmann[3], T. Ruess[3], J. Jelonnek[3]

[1]Uppsala University, Uppsala, Sweden

[2]CERN

[3] Karlsruhe Institute for Technology

Abstract

A coherent detection scheme was tested for dark photons and axion search with millimeter waves. It was shown that relative bandwidth of 169 μHz can be achieved at the center frequency of 30 GHz by commercial equipment. This is in principle a lock-in amplifier at 30 GHz. With a low noise amplifier, thermal noise can be reduced down to 1.36×10^{-24} W with one and half hours data taking and the expected signal was locked within one bin of 169 μHz resolution bandwidth by using the standard 10 MHz reference line. This will lead to a new search of dark photons in the mass range, which is complementary to any previous experiments and a future upgrade project of ALPS-II. Although a fully quantum mechanical argument will be necessary to quantify the ultimate limit of this coherent detection scheme, the use of a state-of-the-art phase-locked gyrotron and superconducting quantum sensors would lead to further improvement of millimeter-wave dark photon and axion searches.

Table of Contents

1. Introduction

Weakly Interacting Slim Particles (WISPs) are hypothetical particles beyond the Standard Model of particle physics and can be dark matter candidates. Amongst all, WISPs interacting with ordinary photons are of interest, namely, Axion-Like-Particles (ALPs) and dark photons. One promising experimental method to search for such WISPs is called Light-Shinning-Through-a-Wall (LSW), in which a very weak photon signal is to be addressed, penetrating through a wall as a form of WISP originally generated by a strong photon source prepared on the other side of the wall. The LSW experiments have been performed in the X-rays [1], optical or infrared light [2, 3] and radiofrequency regions [4]. Different technology was applied to each frequency, and in particular, how to generate and detect photons differentiates these experiments. For example, there are pros and cons in quantum photon detection and classical wave detection. The former has been used for X-rays and optical light experiments because high energy quantum of a photon enables single photon detection. The latter was employed in the radiofrequency experiments but recently single photon sensors have been under development for such a lower frequency range as well.

The frequency range between previous experiments provide a unique opportunity in WISPs search, especially for the dark photons search. The search range of dark photon mass is directly corresponding to the frequency and thus high-frequency microwaves or millimeter waves from 30 GHz to 200 GHz are a niche to address dark photon of mass range 10^{-4} eV as shown in Figure 1 [5]. In this frequency region, high-power photon sources have been developed and would be eventually ready for LSW experiments.

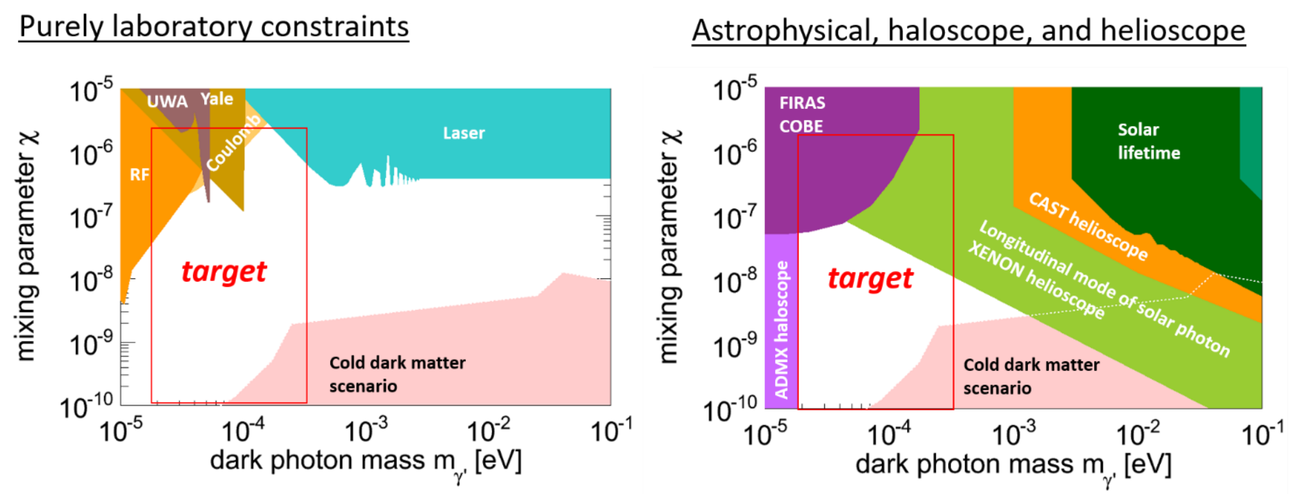

Figure 1 Present constraints

The open question has been about a detection scheme of millimeter waves for LSW. There exist R&D activities for single photon detectors in INFN Pisa and NEST Pisa [6, 7]. It is estimated that the newly developed Josephson Escape Sensor (JES) would show noise equivalent power of the order of 10^{-25} W/√Hz. However, deployment of such a single photon detector still requires substantial investment and is not immediately suitable for testing other components of the LSW experiment at millimeter waves. Instead, in this technical report, we focus on testing a coherent wave detection scheme. This was the method used in the RF LSW experiment from 2009 to 2013 [8, 9] but its application for millimeter waves over 30 GHz was to be demonstrated, because more mixers inside a vector signal analyzer would introduce an additional phase noise. We proved that it is possible to go down to at least the resolution bandwidth of 169 μHz and properly phase locked signal was within one bin of the Fourier transformed spectrum.

2. Millimeter-wave LSW setup and the concept of coherent detection

The conceptual setup of millimeter-wave LSW experiment is shown in Figure 2. In the first stage of the project, a low-power experiment using commercial equipment is planned while the dark photon emitter will be replaced with a high power gyrotron tube in the next step. The setup is composed of 1) dark photon emitter 2) dark photon receiver and 3) signal analyzer for Fourier transform. The emitter is made of a chain of a synthesizer, a solid-state amplifier, and a Fabry-Perot resonator. The receiver is a chain of another Fabry-Perot resonator and a Low-Noise Amplifier (LNA), installed in an EMC shield with around -300 dB separation. The shield is realized by optical fibers for all the feedthroughs including microwaves transmission and even power supplies. The signal analyzer records real time data and performs Fast Fourier Transform (FFT) to integrate out the thermal and white noise from the detection chain.

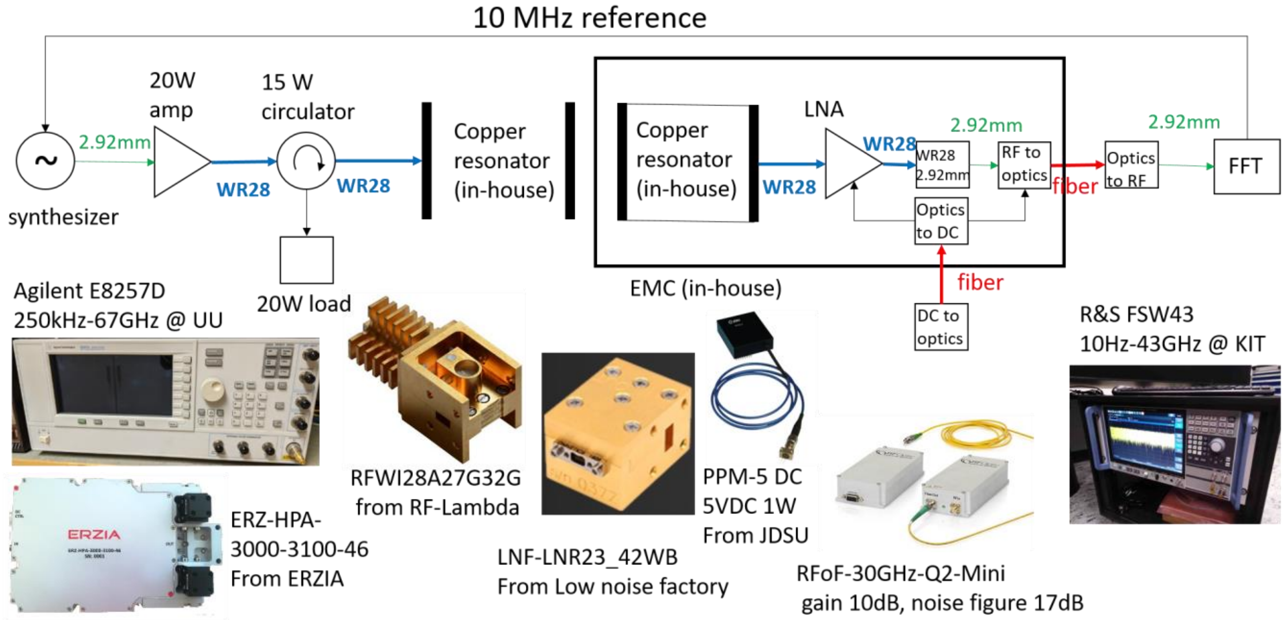

Figure 2 Conceptual setup of millimeter-wave LSW

The benefit of FFT can be understood by the thermal noise power P_N in W:

$$P_N = k_B T_S \frac{\sqrt{\Delta\nu}}{\sqrt{t}},$$

where $k_B = 1.38 \times 10^{-23}$ J/K is the Boltzmann constant, T_S is the system noise temperature in K, $\Delta\nu$ is the resolution bandwidth in Hz, and t is the measurement time in s. In wave detection and FFT with a signal analyzer, $\Delta\nu$ is t^{-1} and therefore P_N is linearly suppressed over a long measurement time t. On the other hand, noise power of incoherent photon detection gains only by $\sqrt{t}$ and thus one needs to cool down T_S for better sensitivity. Table 1 summarizes the noise power of 300 K with different measurement time and corresponding bandwidth. It is clear that data acquisition of longer than 1 second with a signal analyzer, recording the time domain data either in its memory buffer or exporting it to an external device, could address very small noise power or small number of thermal photons. However, the benefit of this method is valid if the expected signal is very coherent and within the extremely narrow bandwidth determined by the FFT. It is mandatory to verify the feasibility of such an extreme coherency at 30 GHz.

Table 1 300 K noise power, bandwidth, and measurement time

t	$\Delta\nu$	P_N	#30 GHz photons/s
100 ms	10 Hz	4.2×10^{-20} W	2100
1 s	1 Hz	4.2×10^{-21} W	200
10 s	100 mHz	4.2×10^{-22} W	21
5 minutes	3 mHz	1.4×10^{-23} W	0.7
1 hour	278 μHz	1.1×10^{-24} W	0.06
1 day	12 μHz	4.8×10^{-26} W	0.002

The trick is *relative* coherency instead of *absolute* coherency. In Figure 2, the FFT device (signal analyzer) and the synthesizer is phase-locked by a standard 10 MHz line. With this scheme, in principle, internal clocks of both emitter and the detector are synchronized and a signal would be ideally a delta function measured by the detector; therefore, the white noise reduction by FFT of $\gg 1$ s is supposed to be very efficient. The question is the ultimate phase stability of phase locking by the common 10 MHz standard. The signal itself is 30 GHz so there exist several up-conversions inside the devices. This gives rise to the suspect that the signal may be slightly smeared but the question is how much it would be. Such a stability of the phase locking determines the maximum integration time at which the gain in signal to noise ratio starts to saturate. We performed a dedicated experiment to check the narrow-band detection scheme.

3. Experimental

We used R&S FSW43 signal analyzer, R&S SMB100A, and Keysight waveform generator 33521A to test the relative coherency of the 10 MHz reference line. A master clock developed for the KARA accelerator also provided absolute 10 MHz reference to the equipment. The experiment was performed in the THz-lab at the KARA accelerator facility in Karlsruhe Institute for Technology as shown in Figure 3.

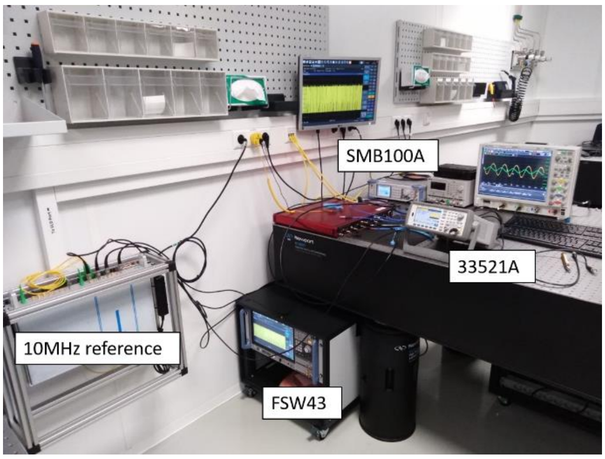

Figure 3 Photograph of experimental setup at THz-lab at KARA

3.1. Response against a ±1 Hz shift in 10 MHz external reference

We first checked the frequency shift in a 30 GHz signal when the 10 MHz external reference was shifted on purpose. Figure 4 shows the two block diagrams for this experiment. In setup 1, the signal generator and the waveform generator were locked by a common reference while the signal analyzer was locked with a deviated 10 MHz reference from the waveform generator. On the other hand, the signal generator was locked by this deviated reference. This test is of critical importance because the influence of the reference signal to the center frequency would depend on multiplication method in each device.

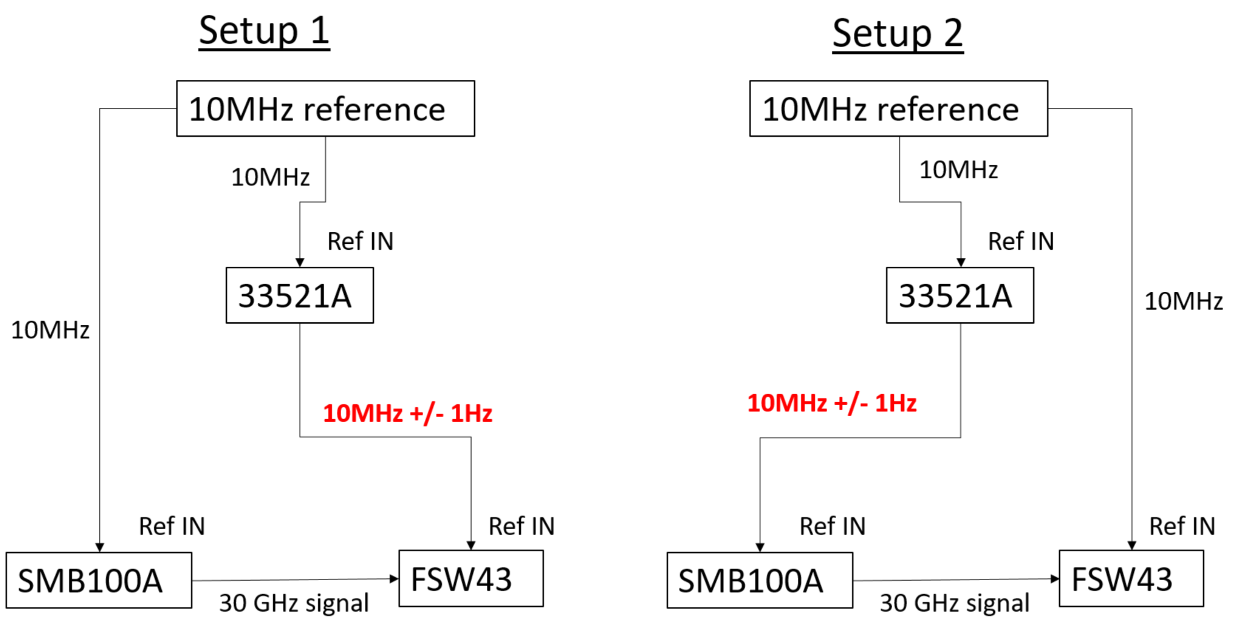

Figure 4 Schematics to check frequency shift by the reference line

Figure 5 and Figure 6 show the results of setup 1 and 2 in Figure 4, respectively. The influence in the frequency shift of center frequency 30 GHz is proportional to the one in reference 10 MHz $\Delta f = f_0 \times \Delta f_{ref}/f_{ref}$ and is 3 kHz. Importantly, the influence in setup 1 and 2 are opposite so that they cancel with each other if the frequency deviation happens in a common reference line to emitter and detector sides.

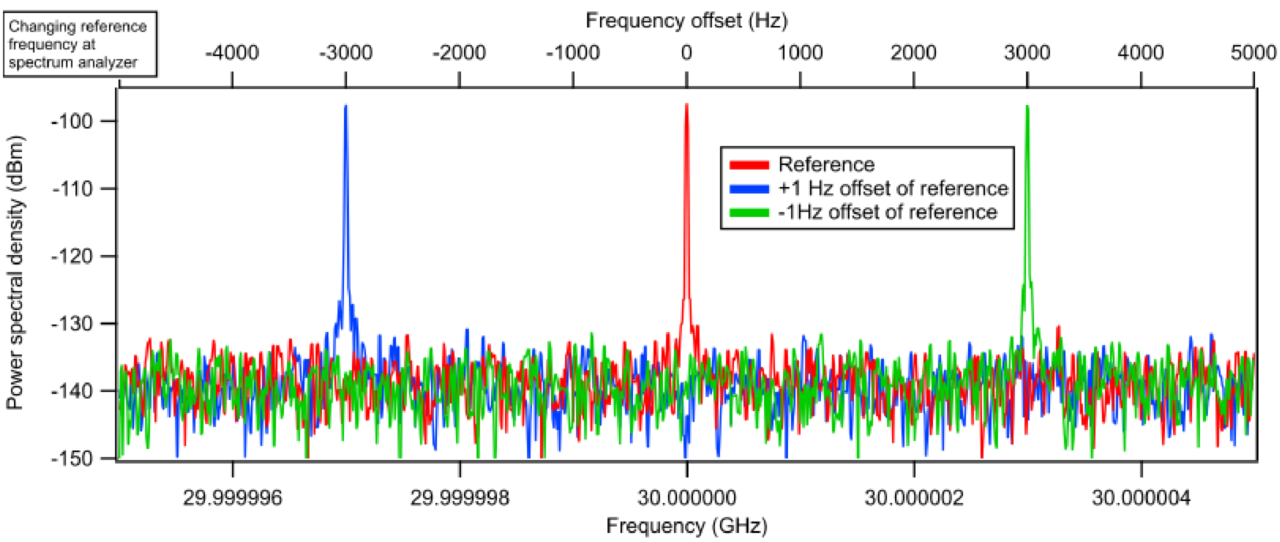

Figure 5 Result of setup 1

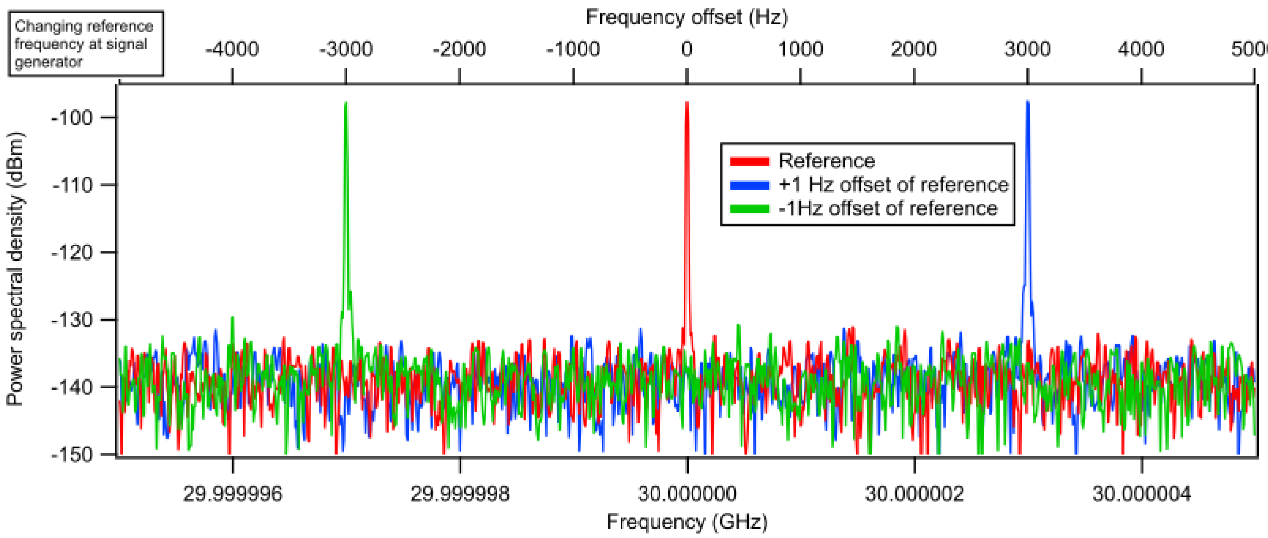

Figure 6 Result of setup 2

3.2. Sub-Hz FFT mode in signal analyzer FSW43

It was tricky to find an option to activate sub-Hz FFT mode in the signal analyzer, because the some functionalities of a general vector signal analyzer are distributed to different software modes in FSW43. The appropriate mode was I/Q analyzer, in which one can select FFT time much longer than 1 s and also reduce resolution bandwidth accordingly. Other modes also offer long integration time but its minimum resolution bandwith was somewhat limited to 100 mHz. The internal memory buffer of 512k in FSW43 offers minimum resolution bandwidth of 169 µHz over one and half hour of data acquisition as shown in Figure 7. Note that "no window" option in the FFT algorithm gave the minimum bandwidth. For even narrower bandwidth, we would need to export the data and perform FFT offline. The purpose of this proof-of-principle test was fulfilled by this default configuration of FSW43.

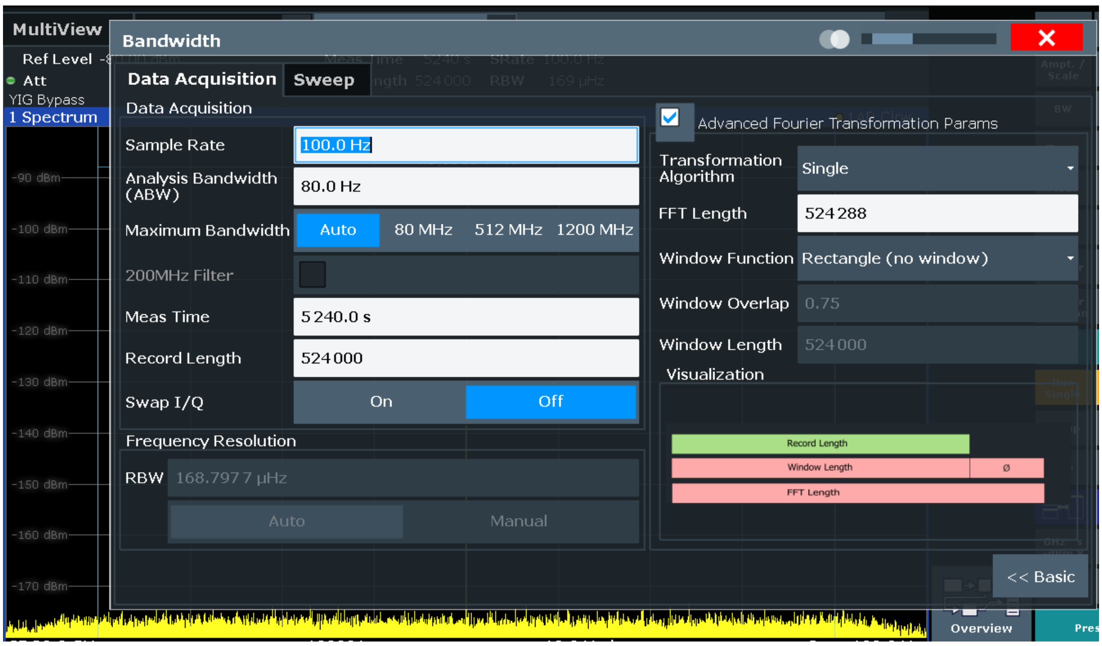

Figure 7 Minimum possible resolution bandwidth in default FSW43

3.3. Narrowband filtering of thermal white noise via FFT

We compared the noise power of five different bandwidths: 1Hz, 100 mHz, 10 mHz, 1 mHz, and 169 μHz, while locking the signal generator and the signal analyzer with a common 10 MHz reference. The intrinsic noise level of FSW43 was around 10^{-17}W/Hz (-140 dBm/Hz) and was worse than the 300 K noise level (-174 dBm). This will be drastically improved by the use of low noise preamplifier of higher than 30 dB as discussed later. Apart from the intrinsic noise level, the noise power was reduced dramatically by narrower bandwidth (or longer FFT) as shown in Figure 8. Figure 9 shows that the reduction of noise power is linear to the bandwidth, just as expected.

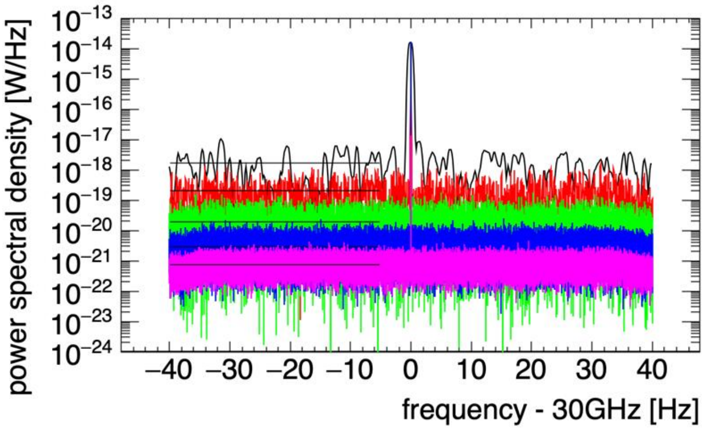

Figure 8 Power spectral density as a function of center frequency for resolution bandwidth of 1 Hz (black), 100 mHz (red), 10 mHz (green), 1 mHz (blue), and 169uHz (magenta). The solid lines show best linear fits.

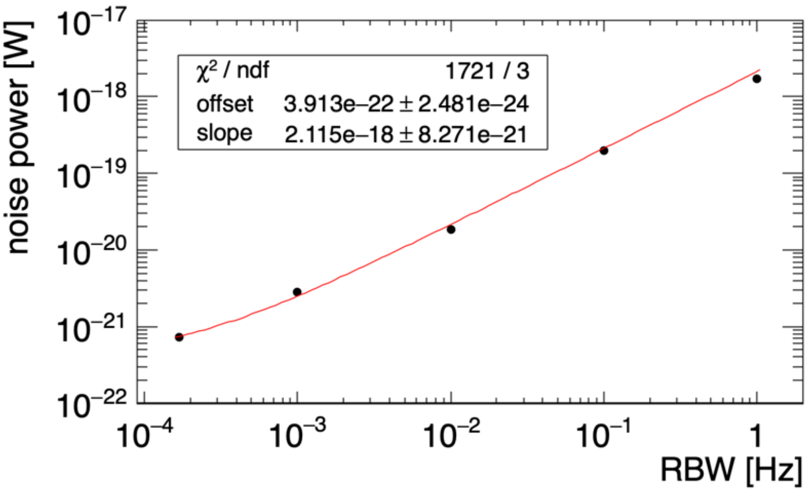

Figure 9 Noise power as a function of resolution bandwidth

3.4. Super-narrow band coherency by the 10 MHz reference

Figure 10 shows the comparison of two signal spectra with an offset correction of 55 Hz for unlocked case. It is clear that the unlocked signal drifted over Hz in 1 hour, which stems from relative fluctuations in the independent signal generator and analyzer. However, once they were locked by the common 10 MHz reference, the signal was stabilized within 1 bin of the spectrum with the resolution bandwidth of 169 μHz. The observed loss at the peak power in this bin was no more than 1 dB.

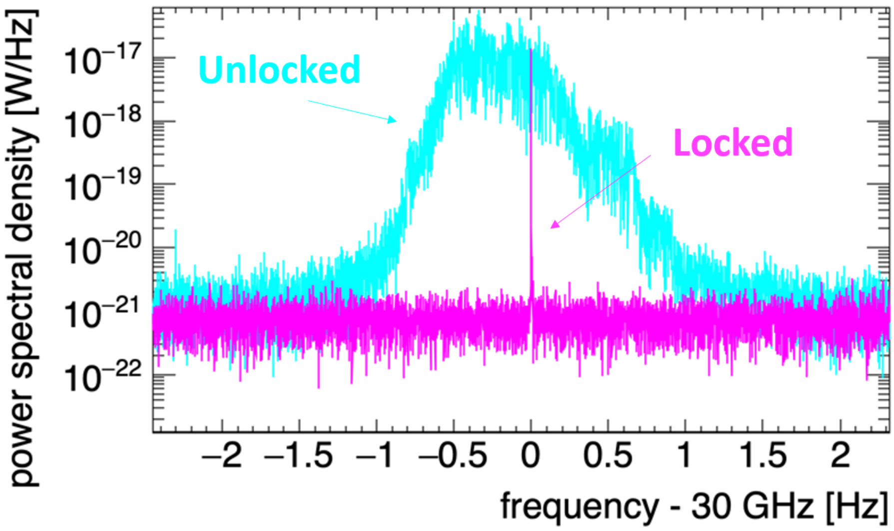

Figure 10 Comparison of signal spectra of locked and unlocked case, both with a resolution bandwidth of 169 uHz. The offset of unlocked case was corrected by hand.

3.5. Absolute stability requirement of the common 10 MHz reference line

The results so far demonstrated that the narrow-band detection scheme would work in 30 GHz and one can reduce the white noise at least four orders of magnitude by integrating the real time signal over more than one hour. A frequency drifts of the emitter and the detector were cancelled out by the common 10 MHz reference. A question arises about the requirement of absolute stability in the 10 MHz reference line. To test this, we added frequency modulation on purpose to the 10 MHz line as shown in Figure 11.

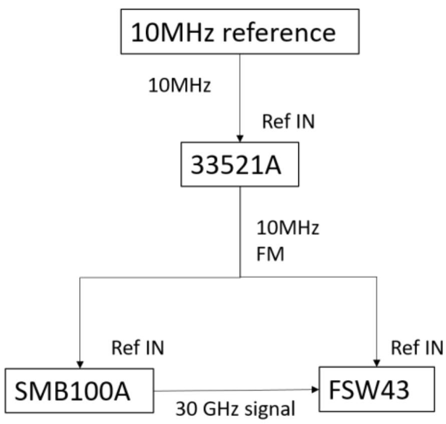

Figure 11 Frequency modulation in the common 10 MHz line

When we added substantial frequency modulation of 1 Hz every 3 seconds on the common 10 MHz reference line, we observed Figure 12, in which the center frequency 30 GHz, relatively obtained by the locked signal generator and the signal analyzer, was also influenced by the perturbation in the reference line. With a certain response time the devices were phase-locked together again. This a very exaggerated case and we expect to have much better stability in standard 10 MHz in any commercial products.

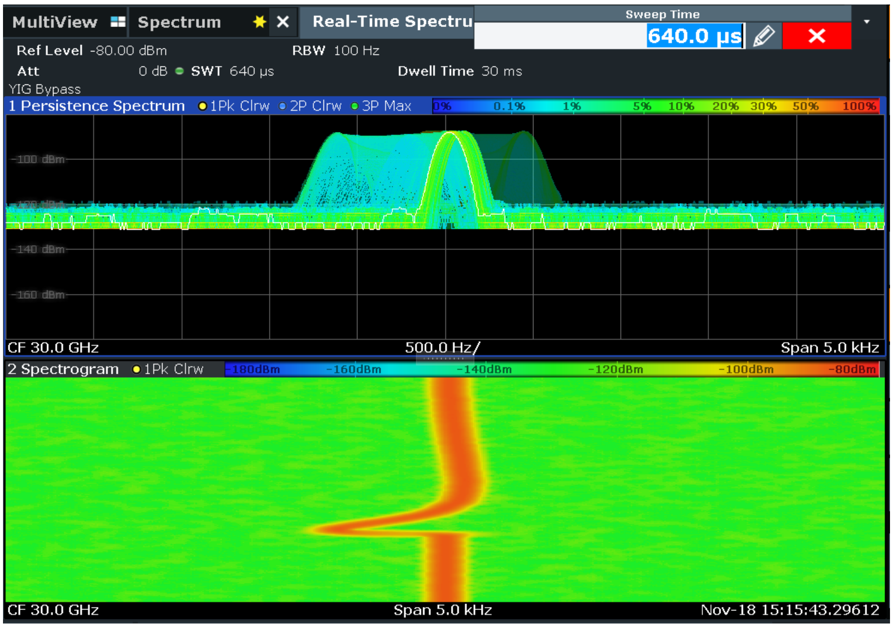

Figure 12 Phase lock response against FM in the 10 MHz line

The waveform generator 33521A offered the minimum FM dev of 1 μHz. Figure 13 compares the two spectra with and without FM dev of 1 μHz and FM frequency of 1 Hz, in case of resolution bandwidth of 169 μHz (FFT integration of over one and half hours). The sideband is slightly larger by this small FM but the influence is marginal. More importantly, this data shows that the absolute stability of the 10 MHz line, just taken from a non-expensive device, is better than FM of 1 μHz and is sufficient to resolve a coherent signal of below the reduced white noise of 10^{-20} W (-170 dBm)

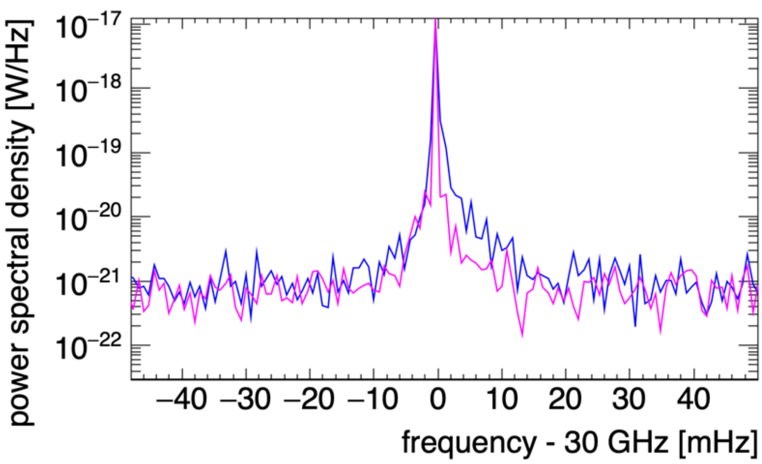

Figure 13 Comparison of no FM (magenta) and 1uHz FM (blue) in the 10 MHz line

4. Discussion

4.1. Further reduction of noise power by an amplifier

In this proof-of-principle test, the noise level of the signal analyzer was around -140 dBm/Hz. This may be a typical value of this type of device without having a preamplifier in the analog frontend. Here, we discuss the benefit of having a low noise preamplifier of around gain 30 dB, which is commercially available around 30 GHz. Let us take LNF-LNR23-42WB from Low Noise Factory. This LNA costs 3300 EUR and has a gain of 31 dB and noise temperature of 110 K with an operation at room temperature. Figure 14 shows the schematic of the preamplifier chain. The signal level is amplified by

$$S = G_1 S_0.$$

On the other hand, the noise level becomes

$$N = G_1(k_B T_0 + k_B T_1) + k_B T_2.$$

The signal to noise ratio is therefore

$$S/N = \frac{S_0}{k_B(T_0 + T_1 + T_2/G_1)}.$$

Comparing with the original S/N without the preamplifier

$$S_0/N_0 = \frac{S_0}{k_B(T_0 + T_2)} \sim \frac{S_0}{k_B T_2},$$

we can reduce the noise by

$$N/N_0 = \frac{T_0 + T_1 + T_2/G_1}{T_2} \sim 0.00136 = -29 \text{ dB}.$$

This is how we can effectively achieve noise power of -169 dB/Hz instead of -140 dB/Hz at the signal analyzer to be reduced down to around -209 dBm (1.36×10^{-24} W or 0.07 photons per second) with the narrow-bandwidth of 169 µHz as shown in this note.

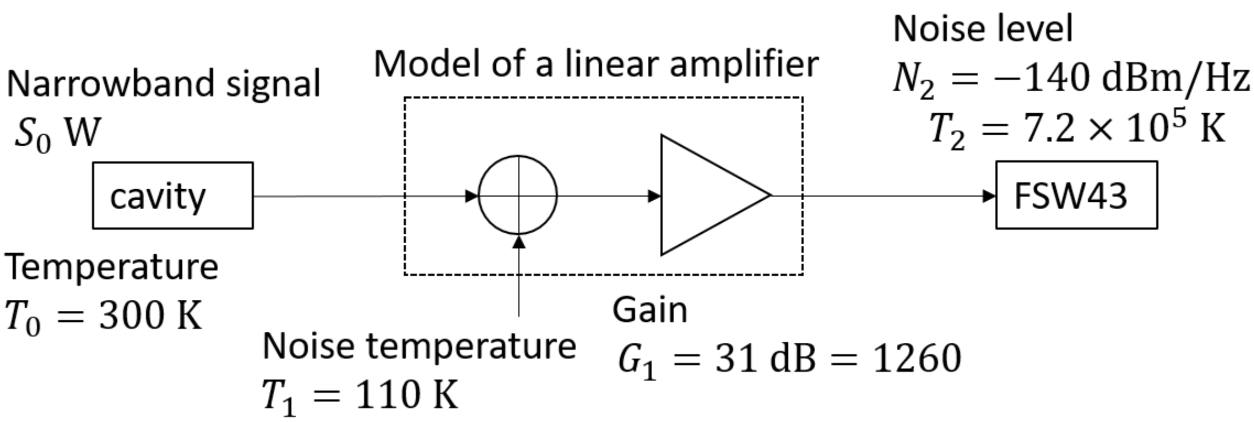

Figure 14 Schematic of an amplifier in this experiment

4.2. Quantum limitation of an amplifier

In order to further reduce the noise power, one can cool down the cavity $(T_0 = 300\text{K} \rightarrow 4\text{K})$ and a cryogenic amplifier (for instance LNF-LNC23_42WB; $G_1 = 28$ dB; $T_1 = 9.4$ K; operated at 5K) as well as adding another preamplifier with gain G_2 to suppress the noise level of the signal analyzer (T_2/G_1G_2). It is possible that one exports the signal analyzer's real time data and applies FFT off-line over one day, which would lead to the resolution bandwidth of $10\ \mu\text{Hz}$. By this strategy, we may be able to reduce the noise level by other three orders of magnitude, such as -239 dBm (1.36×10^{-25} W or 7×10^{-5} photons per second).

A fundamental question about an amplifier is its minimum noise level. Classical electrodynamics is no longer valid if the number of photons is approaching to single photon level or even lower. Naively, an intrinsic noise caused by quantum fluctuations would limit the minimum possible signal level for linear amplification.

The so-called standard quantum limit of a linear amplifier is given by twice the zero point energy of the input state [10]:

$$k_B T_{SQL} \sim 2 \times \frac{h\nu}{2} \sim 2 \times 10^{-23}\ \text{W/Hz}$$

for $\nu = 30$ GHz photons. This corresponds to $T_{SQL} = 1.4$ K but a commercial amplifier of 30 GHz range is currently blocked above this level. A parametric amplifier could reach T_{SQL} but is not immediately ready for 30 GHz. Anyhow, the minimum possible power resolved by the coherent scheme with a linear amplifier is

$$P_{SQL} = k_B T_{SQL} \frac{\sqrt{\Delta\nu}}{\sqrt{t}} = \frac{k_B T_{SQL}}{t}.$$

The method presented in this report can linearly decrease the noise power by integrating the data for even longer time, down to 10^{-28} W with such a quantum limited coherent detection.

5. Conclusion and outlook

Based on the results of this proof-of-principle test, we can make a conservative guess of search range of the dark photon at low power. If we assume two Fabry-Perot cavities of finesse 3000 (loaded quality factor of around 3×10^4) at 300 K, with a power amplifier of 20 W, a low noise amplifier with gain of 31 dB and noise figure of 110 K, FFT by the signal analyzer down to resolution bandwidth of 169 μHz (one and half hour of measurement time), we can obtain the search range as shown in Figure 15. Here, the geometrical coupling between two Fabry-Perot cavities is estimated by plane-wave approximation which is not strictly valid when the photon dark photon mass is close to the photon energy. Moreover, some insensitive regions in the dark photon mass were smeared by three set of different experiments by chancing the length of Fabry-Perot resonators by ± 10 %. It is important to note that the expected search range is complementary to all the previous experiments and future ALPS-IIb upgrade with 100 m cavities for infrared lasers.

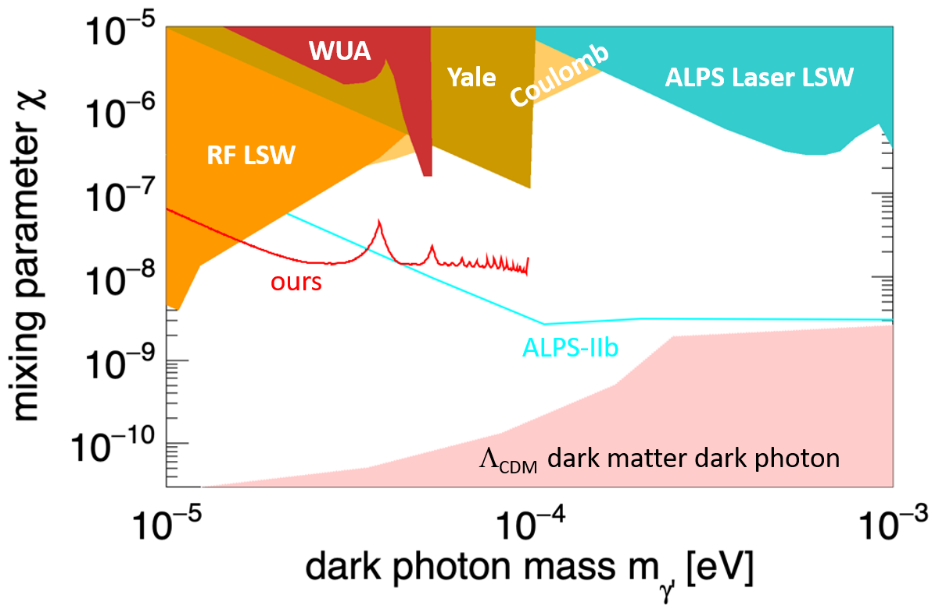

Figure 15 Expected search range of low power narrow-band experiment

In order to enhance the sensitivity of the dark photon search, we can consider following developments.

1. Deployment of a high-power narrow-band grytoron

It is demonstrated that a gyrotron of CW 20 kW output can show absolute signal bandwidth of 1 Hz by using phase-lock loop in the modulation anode [11]. With a very stable cathode modulator, it would be possible to achieve relative bandwidth of sub-Hz with a similar method as shown in this note. Together with a high-power quasi-optical resonator, developed in other applications, we can enhance the sensitivity by one order of magnitude. The overview of high-power source and cavities deserve another report.

2. Deployment of superconducting single photon sensors

It is shown that newly developed Josephson Escape Sensor operated under 100 mK can show noise equivalent power of $10^{-25}\,\mathrm{W}/\sqrt{\mathrm{Hz}}$ [7]. This can avoid the standard quantum limit in the coherent detection and provides a potential breakthrough, in particular, frequency higher than 30 GHz, such as 170 GHz. With this sensor and a gyrotron, we may be able to search for dark matter region shown in Figure 15.

Acknowledgements

This study was supported by the International Excellence Fellowship program in Karlsruhe Institute for Technology in 2021. We would like to thank Elena Pfeifer and Petra Roth for supporting this project.

References

[1] T. Inada, et al., PLB, 722, 301-304 (2013)

[2] K. Ehret, et al., (ALPS collaboreation) Phys. Lett. B, 689, 149-155 (2010)

[3] R Bähre, et al. (ALPS collaboration), JINST 8 T09001 (2013)

[4] M. Betz, et al. (CROWS collaboration) Phys. Rev. D 88 075014 (2013)

[5] A. Miyazaki and P. Spagnolo, arXiv:2008.09223

[6] F. Paolucci, et al., Journal of Applied Physics 128, 194502 (2020)

[7] F. Paolucci, et al., Phys. Rev. Appl. 14 3 034055 (2020)

[8] F. Caspers, S. Federmann, and D. Seebacher, CERN-BE-Note-2009-026

[9] F. Caspers, J. Jaeckel, and R. Ringwald, arXiv:0908.0759, published in JINST

[10] S.K. Lamoreaux et al Phys Rev D 98 035020 (2013)

[11] Tsvetkov A.I. et al "Progress in the development of ultra-stable gyrotrons for spectroscopy and plasma applications", The national Workshop on Far-Infrared Technologies (IW-FIRT 2021), March 8-9, 2021